Patched controls the Hedgehog gradient by endocytosis in a dynamin-dependent manner, but this internalization does not play a major role in signal transduction

Carlos Torroja, Nicole Gorfinkiel and Isabel Guerrero*

Centro de Biología Molecular 'Severo Ochoa', CSIC, Universidad Autónoma de Madrid, Cantoblanco, E-28049 Madrid, Spain
*Author for correspondence (e-mail: iguerrero@cbm.uam.es)

Accepted 13 January 2004

Development 131, 2395-2408
Published by The Company of Biologists 2004
doi:10.1242/dev.01102

Summary

The Hedgehog (Hh) morphogenetic gradient controls multiple developmental patterning events in *Drosophila* and vertebrates. Patched (Ptc), the Hh receptor, restrains both Hh spreading and Hh signaling. We report how endocytosis regulates the concentration and activity of Hh in the wing imaginal disc. Our studies show that Ptc limits the Hh gradient by internalizing Hh through endosomes in a dynamin-dependent manner, and that both Hh and Ptc are targeted to lysosomal degradation. We also found that the ptc^{14} mutant does not block Hh spreading, as it has a failure in endocytosis. However, this mutant protein is able to control the expression of Hh target genes as the wild-type protein, indicating that the internalization mediated by Ptc is not required for signal transduction. In addition, we noted that both in this mutant and in those not producing Ptc protein, Hh still occurred in the endocytic vesicles of Hh-receiving cells, suggesting the existence of a second, Ptc-independent, mechanism of Hh internalization.

Key words: Hedgehog signaling, Patched, Morphogenetic gradients, Dynamin, Deep Orange

Introduction

The formation of morphogenetic gradients is a recurring event during development. In *Drosophila*, the morphogens Wingless (Wg), Decapentaplegic (Dpp) and Hedgehog (Hh) are secreted from localized sources and determine, in a dose-dependent manner, the fate of cells several cell diameters away (reviewed by Vincent and Dubois, 2002). Three processes can affect the extension and slope of a morphogen gradient: the rate of production at the source, the rate of transport, and the rate of degradation. The mechanism by which these gradients form remains controversial. Yet despite theoretical and experimental studies supporting the idea that morphogen gradients can form by diffusion through the extracellular matrix (reviewed by Lander et al., 2002), it has been proposed that morphogens spread through repeated cycles of endocytosis and exocytosis, a process called transcytosis (Entchev et al., 2000; Greco et al., 2001). Furthermore, there is increasing evidence that endocytosis regulates the concentration and therefore the extension of morphogen activity (reviewed by Seto et al., 2002). It has been also recently proposed that self-enhanced ligand degradation underlies robustness of morphogen gradients (Eldar et al., 2003). Thus, Wg internalization and degradation modulate its asymmetric gradient in embryonic segments (Dubois et al., 2001) and also regulate the Wg gradient in wing imaginal discs (Strigini and Cohen, 2000). It is known that receptors play a central role in regulating endocytic trafficking. Hence, the morphogen receptor must also have a role in shaping the morphogen gradient. There are reports that altering the levels of the Dpp receptor, Thickvein, affects Dpp distribution (Lecuit and Cohen, 1998; Entchev et al., 2000).

The wing imaginal disc consists of a single-layered sac of polarized epithelial cells with their apical surfaces orientated towards the disc lumen. In this epithelium, two populations of cells with different adhesion affinities divide the field into posterior (P) and anterior (A) cells (García-Bellido et al., 1973). The Hh protein synthesized by the P cells is released and reaches the cells in the A compartment (Ingham and McMahon, 2001). However, just how Hh reaches cells distant from its site of synthesis, and how its concentration gradient is regulated, is not known. Hh signaling requires the activity of two transmembrane proteins: Patched (Ptc), the Hh-receptor and Smoothened (Smo), the activator of the Hh pathway. In the absence of Hh, Ptc downregulates the activity of Smo. It has been suggested that Ptc increases Smo turnover when they meet in the same subcellular compartment (Denef et al., 2000; Incardona et al., 2002). In addition, it has been proposed that internalization of Hh by Ptc changes the subcellular localization of Ptc, preventing Smo degradation and activating Hh signaling (Denef et al., 2000). This Hh pathway activation leads to further expression of *ptc*, which in turn restricts the range of Hh transport. So, Ptc has two roles: to activate Hh signaling and to sequester Hh as genetic studies in *Drosophila* have shown (Chen and Struhl, 1996). Ptc is a membrane protein with 12 transmembrane domains homologous to sterol-sensing-domain (SSD)-containing proteins (reviewed by Kuwabara and Labouesse, 2002). The sterol-sensing domain of Ptc is involved in Hh signaling but not in Hh sequestration, and it has been proposed to modulate Smo activity through vesicular trafficking (Martín et al., 2001; Strutt et al., 2001). The second function of Ptc, Hh sequestration, appears to

regulate the Hh morphogenetic gradient (Tabata and Kornberg, 1994; Chen and Struhl, 1996; Martín et al., 2001; Strutt et al., 2001). Hitherto, it was believed that Hh effectively promoted its own sequestration (reviewed by Ingham and McMahon, 2001) by upregulating *ptc* transcription. This negative feedback mechanism restrains the range of Hh signaling. However, the cellular mechanisms by which Ptc controls the Hh gradient remain unclear.

We investigated the role of Ptc-mediated endocytosis in the control of Hh gradient formation and signaling in the A compartment of the wing imaginal disc. Our data show that Ptc limits the Hh gradient by internalizing Hh through endosomes in a dynamin-dependent manner and that this Hh-Ptc complex is targeted to degradation by lysosomes. We have genetically uncoupled the two proposed functions of Ptc, through the analysis of the ptc^{14} mutant that is unable to sequester Hh and yet retains a normal capacity to mediate Hh signaling. Our analysis leads to the suggestion that Hh signaling can occur in the absence of Ptc-mediated Hh internalization.

Materials and methods

Fly stocks

Description of mutations, insertions and transgenes in FlyBase are available at http://gin.ebi.ac.uk:7081.

Chromosomes used were as follows.

FRT42D

P {ry[+t7.2]=neoFRT}42D arm-lacZ
P {ry[+t7.2]=neoFRT}42D P{Ubi-GFP(S65T)nls}

FRT18A

w[1118] P{Ubi-GFP(S65T)nls} P{neoFRT}18A
w[1118] arm-lacZ P{neoFRT}18A

Flipase

Hsp70-flipase chromosomes were provided by G.Struhl.

The amorphic ptc^{16} (also known as ptc^{IIW109}) allele, the embryonic lethal alleles ptc^{S2} and ptc^{14} (also known as ptc^{IIR87}) were from Tübingen (Nüslein-Volhard and Wieschaus, 1980).

In addition, the null dor^{8} allele (Shestopal et al., 1997) and the temperature-sensitive, shi^{ts1} (Grigliatti et al., 1973) and hh^{ts2} (Ma et al., 1993) alleles were used. The restrictive temperatures for the shi^{ts1} and hh^{ts2} alleles are 32°C and 29°C, respectively.

The reporter genes used were *dpp-LacZ*$^{BS\ 3.0}$, expressed as the endogenous RNA in the imaginal disc (Blackman et al., 1991); dpp^{10638} (a *dpp* mutant with a *lacZ* insertion) (Zecca et al., 1995); and *ptc-lacZ* (a *lacZ* insertion in the *ptc* gene), which was a gift from C. Goodman.

The *Gal4* drivers for ectopic expression experiments using the *Gal4/UAS* system (Brand and Perrimon, 1993) were the following: *c765-Gal4* [ubiquitously expressed in the wing disc (Nellen et al., 1996)], *ptc-Gal4* (a gift from J. Campos-Ortega), *hh-Gal4* (a gift from T. Tabata) and *AB1-Gal4* (Munro and Freeman, 2000).

Genotypes of larvae for generating mosaic clones

Mutant clones

Clones were generated by *FLP*-mediated mitotic recombination. Larvae of the corresponding genotypes were incubated at 37°C for 1 hour at 24-48 hours after egg laying (AEL), or for 45 minutes at 48-72 hours AEL. The genotypes of the flies for clone induction were:

y, w, FLP/+; en-Gal4 / UAS-HhGFP; FRT82 arm-lacZ / FRT82B $disp^{S037707}$
shi^{ts1} *FRT18A / arm-lacZ FRT18A; FLP/+*
shi^{ts1} *FRT18A / arm-lacZ FRT18A; FLP; hh-Gal4 / HhGFP*
shi^{ts1}*; FRT42D* ptc^{16} */ FRT42D ubi-GFP; FLP/+*
shi^{ts1}*; FRT42D* ptc^{14} */ FRT42D ubi-GFP; FLP/+*
dor^{8} *FRT18A / arm-lacZ FRT18A; FLP/+*
dor^{8} *FRT18A / ubi-GFP FRT18A; dpp-lacZ/+; FLP/+*
dor^{8} *FRT18A / ubi-GFP FRT18A; ptc-lacZ/+; FLP/+*
FLP122/+; FRT42D ptc^{14} */FRT42D arm-Lac-Z*
FLP122/+; FRT42D ptc^{14} */* dpp^{10638} *FRT42D ubi-GFP*
FLP122/+; FRT42D ptc^{14} */ FRT42D arm-lacZ;* hh^{ts2}
FLP122/+; FRT42D ptc^{14} */ FRT42D arm-lacZ; hh-Gal4 / HhGFP*
FLP122/+; FRT42D ptc^{16} */ FRT42D arm-lacZ; hh-Gal4 / HhGFP*

Flip-Out clones

To generate random clones of wild-type $ptc^{WT}GFP$, $ptc^{14}GFP$ and *hhGFP*, the *actin>CD2>Gal4* (Pignoni and Zipursky, 1997) or *ubx>*f^{+}*>Gal4, UAS-*β*gal* (de Celis and Bray, 1997) transgene was used. Larvae of the corresponding genotypes were incubated at 37°C for 15 minutes to induce *HS-FLP*-mediated recombinant clones.

Act>CD2>GAL4 / HS-FLP122; $ptc^{WT}GFP$
Act>CD2>GAL4 / HS-FLP122; $ptc^{14}GFP$
y, w, HS-FLP122; ubx>f^{+}*>Gal4, UAS-*β*gal/ UAS-HhGFP*

Transgenes

Hh transgene

For the HhGFP fusion protein, the GFP-coding sequence was amplified by PCR from a pEGFP-N1 vector (Clontech, catalog number 6085-1) and tagged in frame before cleavage site of Hh by auto-proteolysis (…SH254-GFP-V255HGCF…) (Fig. 1A).

Ptc transgenes

To obtain the Ptc^{14} mutation (L83Q), the QuickChange™ Site-Directed Mutagenesis Kit (Stratagene) was used to introduce a point mutation into the *ptc* cDNA (T242A). This was confirmed by sequence analysis. The GFP-tagged proteins of ptc^{S2}, ptc^{WT} and ptc^{14} were cDNA fusions cloned in frame by PCR into a *pEGFP-N1* vector (Clontech, catalog number 6085-1). The GFP sequences were tagged in frame to the C-terminal regions of both Ptc^{WT} and Ptc^{14}. The stop codon was substituted by a glycine (codon 1287), followed by a valine (codon 1288) and the first methionine of the GFP sequence (Fig. 2A). *ptcGFP* fusions were transferred to the *pUAS* vector. Several transgenic lines were obtained. Experiments involving the three Ptc protein forms (wild-type and mutant forms) were conducted using the transgenic fly lines that showed similar levels of Ptc expression after induction with the same Gal4 line.

Other transgenic flies

UAS-Rab7GFP (Entchev et al., 2000).
UAS-ptc^{S2} (Martín et al., 2001).

Functional characterization of HhGFP fusion protein

It was expected that the fusion of the GFP sequence to Hh cDNA at position between codons 254 (H) and 255 (V) did not interfere neither with the processing, secretion and diffusion process of Hh nor with the Hh binding to Ptc (Burke et al., 1999; Pepinsky et al., 2000). To determine whether the auto-proteolysis of HhGFP occurs normally, we analyzed the presence of the distinct species of Hh by western blot using either anti-Hh (Tabata and Kornberg, 1994) or anti-GFP antibodies (Fig. 1B). In the salivary gland extracts from *AB1-Gal4*/*UAS-Hh* flies, three bands of ~45 kDa (U in Fig. 1B, row 1; uncleaved Hh), 25 kDa (C in Fig. 1B, row 1; C-terminal half of Hh) and 20 kDa (N in Fig. 1B, row 1; N-terminal active form) were observed using anti-Hh antibody as it was previously reported (Lee et al., 1994; Tabata and Kornberg, 1994; Porter et al., 1995). Three major bands were also observed in salivary glands extracts from *AB1-Gal4*/*UAS-Hh* GFP flies using either anti-Hh or anti-GFP antibodies. The molecular weight of these bands corresponded to the ones expected for the un-cleaved HhGFP chimera (70 kDa, U in Fig. 1B,

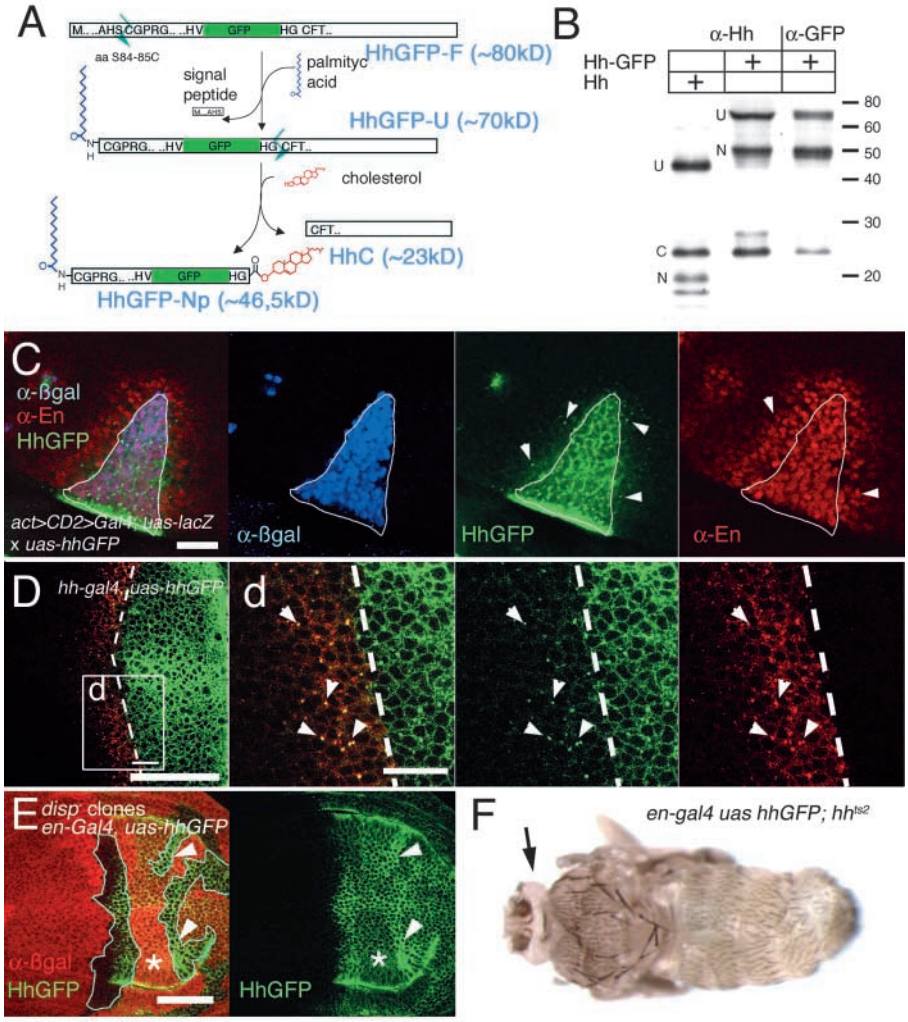

Fig. 1. The HhGFP chimera behaves as the wild-type Hh protein. (A) Scheme of the predicted HhGFP fusion protein processing. HhGFP-F, full-length protein; HhGFP-U, the unprocessed protein without the signal peptide; HhC, the C-terminal region of the processed protein; HhGFP-Np, the N-terminal region of the processed protein with the GFP fragment and the palmitic acid and cholesterol modifications. (B) Western blot of protein extracts from *AB1-Gal4/UAS-Hh* and *AB1-Gal4/UAS-HhGFP* salivary glands stained with anti-Hh or anti-GFP. U, unprocessed protein (HhU); N, processed protein (HhNp); C, catalytic fragment (HhC). (C) Ectopic clones of HhGFP (green) in A cells (labeled by β-Gal staining, blue) of a wing imaginal disc stained with anti-En (red). Ectopic expression of HhGFP in A wing pouch cells is able to induce En expression inside the clone and non-autonomously in a region of three to four cell diameters around the clone (arrowheads in red panel) as wild-type Hh. Note that HhGFP vesicles are detected in cells far from the source (arrows in green panel). (D) *hh-Gal4/UAS-HhGFP* wing imaginal disc stained with anti-Ptc (red). (d) Magnification of the boxed area in D. HhGFP signal is observed in A cells co-localizing with Ptc protein in vesicles (arrowheads). (E) *disp*$^{-}$ clones (labeled by the lack of β-gal staining, red) in a *en-Gal4/UAS-HhGFP* (green) wing imaginal disc. There is an accumulation of Hh-GFP in the *disp*$^{-}$ mutant cells (arrowheads) with respect to the wild-type region (asterisk). (F) *en-Gal4/UAS-HhGFP; hh*^{ts2} pharate raised at restrictive temperature during larvae development. All the structures were rescued except for some head structures (arrow) where the expression of *en* depends on Hh expression. In this and all other figures, the A compartment of the wing disc is towards the left and the P is towards the right. A broken line indicates the AP compartment border. Scale bars: 15 μm in C,d; 50 μm in D,E.

rows 2 and 3), for the HhGFP-Np (46 kDa, N in Fig. 1B, rows 2 and 3) and for the HhC (25 kDa, C in Fig. 1B, row 2), indicating that the Hh-GFP processing occurs normally.

To assay if HhGFP is secreted and spread normally we analyzed the effect of ectopic HhGFP expressing clones in the wing imaginal disc. In the A compartment of the wing pouch, these clones were able to induce En expression autonomously and non-autonomously (Fig. 1 C) as does the wild type Hh protein (Basler and Struhl, 1994; Zecca et al., 1995). Co-localization of Ptc and HhGFP in vesicles was observed in the A cells close to the AP border in an *hh-Gal4/UAS-Hh* wing disc (Fig. 1D,d).

To test if HhGFP was modified by cholesterol we induced *dispatched (disp*$^{-}$*)* mutant clones in an *en-Gal4/UAS-HhGFP* wing disc. It has been reported a membrane accumulation of Hh-Np in the absence of Disp that is dependent on its cholesterol modification (Burke et al., 1999). As it was expected, *disp*$^{-}$ clones induced in the P compartment showed an autonomous accumulation of Hh-GFP compared with the wild-type territory (Fig. 1E). This result indicates that HhGFP-Np is cholesterol modified.

Finally, to determine if HhGFP can substitute the endogenous function of Hh, we performed rescue experiments of the *hh* mutant phenotype. *hh*^{ts2} flies raised at the restricted temperature (29°C) during the larvae period to the end of development are lethal. However, *en-Gal4/UAS-HhGFP; hh*^{ts2} mutant flies raised at the restricted temperature (29°C) for the same developmental period were rescued to pharates showing normalized notum, legs, abdomen and genitalia (Fig. 1F). The wings were present but not extended. In the head, some structures were rescued but the dorsal head, the ocelli and the eyes were not rescued probably because *en* expression begins after the on set of *hh* expression (Royet and Finkelstein, 1997). These results indicate that HhGFP is able to substitute the wild-type Hh function.

Functional characterization of PtcGFP fusion proteins

To characterize the PtcGFP fusion proteins first, we analyzed the integrity of the fusion proteins by western blot. We detected the presence of a protein band of 180 to 200 kDa approximately in extracts of *AB1-Gal4/UAS-Ptc*^{WT}*GFP* or *UAS-Ptc*^{14}*GFP* salivary glands using the anti-GFP antibody (Fig. 2B). This band has a molecular weight higher than the expected 16,964 kDa based on DNA sequence, probably because Ptc has six potential glycosylation sites.

Then, we assayed the ability of the Ptc^{WT}GFP fusion protein to sequester Hh when it was expressed in the P compartment. Ectopic expression of the wild-type Ptc in the P compartment reduces the range of Hh signaling (Johnson et al., 1995) and induces the accumulation of Hh (Martín et al., 2001). The expression of Collier, one of the Hh targets, was reduced when Ptc^{WT}GFP was overexpressed in the P compartment (Fig. 2D). In addition, ectopic

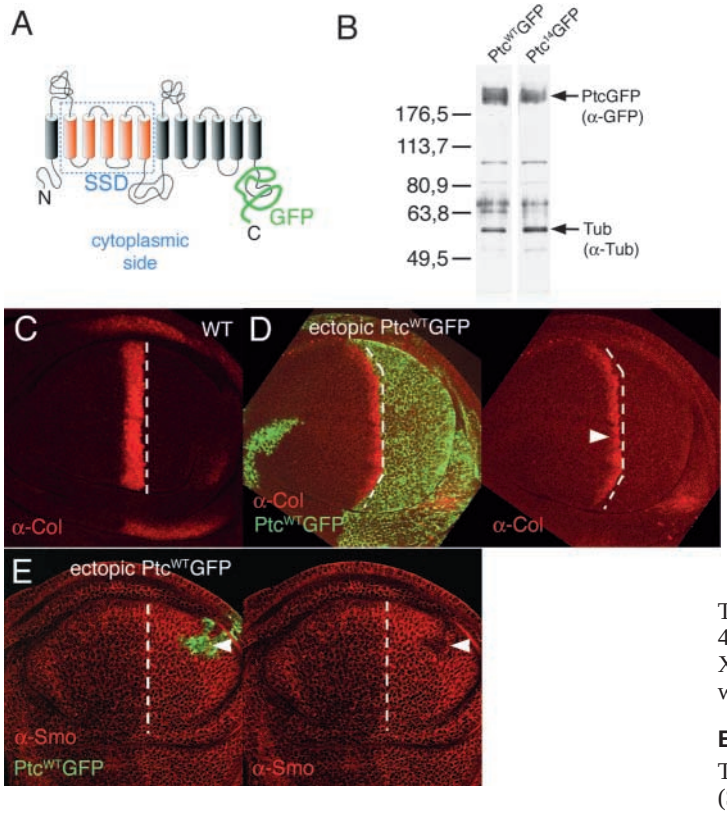

Fig. 2. The Ptc^{WT}GFP chimera behaves as the wild-type Ptc protein. (A) Scheme of the PtcGFP fusion protein. The GFP is tagged to the C-terminal cytoplasmic tail of Ptc. (B) Western blot of protein extracts from *AB1-Gal4/UAS-Ptc^{WT}GFP* or *AB1-Gal4/UAS-Ptc^{14}GFP* salivary glands stained with anti-GFP and anti-Tubulin. Both Ptc^{WT}GFP and Ptc^{14}GFP proteins migrate with an apparent molecular weight of 180-200 kDa. (C) Collier (Col) expression pattern in a wild-type wing imaginal disc. (D) A large ectopic Ptc^{WT}GFP clone in the P compartment causes a reduction of Col expression (arrowhead) at the AP compartment border because of the sequestration of Hh by the ectopic Ptc (see also Fig. 7A). (E) An ectopic Ptc^{WT}GFP clone in the P compartment of a wing imaginal disc stained with anti-Smo (red). Note the autonomous downregulation of Smo because of the repressive activity of Ptc (arrowheads).

Ptc^{WT}GFP clones in the P compartment induced an autonomous accumulation of Hh (see Fig. 7A). Finally, we observed a downregulation of Smo in Ptc^{WT}GFP ectopic clones in the P compartment (Fig. 2E) as it has been reported for the wild type Ptc (Denef et al., 2000; Martín et al., 2001). Collectively, these data indicate that Ptc^{WT}GFP behaves as the wild-type protein.

Immunostaining of imaginal discs and western blot analysis

Immunostaining was performed following standard protocols. Antibodies were used at the following dilutions: rabbit polyclonal anti-Hh 1/400 (raised for the present study), rat polyclonal anti-Hh 1/100 (Sánchez-Herrero et al., 1996), mouse monoclonal anti-Ptc (Apa 1.3) (Capdevila et al., 1994b) 1/100, rabbit polyclonal anti-β-gal (Jackson Laboratories) 1/1000, rabbit polyclonal anti-GFP (Molecular Probes, catalog number A-6455) 1/100, rabbit polyclonal anti-Col antibody (Vervoort et al., 1999) 1/200, mouse monoclonal anti-En (Patel et al., 1989) 1/10, mouse monoclonal anti-Wg (Brook and Cohen, 1996) 1/50, rat polyclonal anti-Smo (Denef et al., 2000) 1/200, rat monoclonal anti-Ci (Motzny and Holmgren, 1995) 1/10 and rat polyclonal anti-Caupolican (Diez del Corral et al., 1999) 1/1000, Stained imaginal discs were examined using a BioRad confocal laser-scanning microscope.

For western blot analysis, protein extracts from salivary glands of *AB1-Gal4/UAS-Hh*, *UAS-HhGFP*, *UAS-Ptc^{WT}GFP* or *UAS-Ptc^{14}GFP* flies were prepared in Laemmli buffer and resolved by SDS-PAGE, immunoblotted and then analyzed using anti-Hh (1/500) (Tabata and Kornberg, 1994) and anti-GFP (1/1000) (Molecular Probes, catalog number A-6455) antibodies. Horseradish peroxidase-conjugated secondary antibodies were used to develop the signal using the ECL Western Blotting Analysis System (Amersham Pharmacia).

Labeling the endocytic compartment

Third instar larval discs were incubated in 3.7 mM Red-dextran (lysine fixable, MW3000; Molecular Probes) in M3 medium at 25°C (pulse) and then washed five times for 2 minutes in ice-cold M3 medium. The discs were then incubated for a chase period at 25°C in M3 medium prior to fixation in 4% paraformaldehyde. To visualize the early endosomes of the endocytic compartments, the discs were pulsed for 5 minutes without a chase period. For late endosomes, a 5 minutes pulse and 60 minutes chase were used. This was followed by fixing in PBS 4% paraformaldehyde (PF) for 40 minutes at 4°C and in 4% paraformaldehyde in PBS 0.05% Triton X-100 for 20 minutes at room temperature. The discs were then washed and incubated with antibodies in PBS 0.05% Triton X-100.

Extracellular labeling of HhGFP in *shi^{ts1}* mutant clones

This protocol was modified from that described by Strigini and Cohen (Strigini and Cohen, 2000). Larvae containing *shi* mutant clones where maintained at restrictive temperature (32°C) for 3 hours, dissected at restrictive temperature and transferred immediately to ice-cold M3 medium containing anti-GFP antibody. They were then incubated at 4°C for 30 minutes, washed in ice-cold PBS and fixed in PBS 4% PF at 4°C. By transferring the discs from 32°C to ice-cold medium, the cells stop their vesicular trafficking and the proteins remain at their subcellular locations at the moment of cooling. Incubating with the anti-GFP antibody under these 'in vivo' conditions, without detergents and prior to fixation, rendered the antibody incapable of penetrating the cells. Thus, only extracellular antigen was labeled. The antibody does not label intra-cellular HhGFP. The lack of staining of the intracellular HhGFP vesicles in the P compartment of the same disc (see Fig. 3b, arrows) was used as a control for this specific extracellular anti-GFP antibody staining method.

Extracellular labeling of Ptc in ectopic Ptc^{WT}GFP and Ptc^{14}GFP clones

Larvae containing ectopic Ptc^{WT}GFP and Ptc^{14}GFP clones were dissected and incubated in ice-cold medium with anti-Ptc antibody at 1/10 dilution in M3 medium for 30 minutes, washed with ice-cold PBS and fixed with 4% paraformaldehyde for 20 minutes at 4°C and 20 minutes at 25°C. After fixation, discs were incubated with the corresponding secondary antibody.

Quantification analysis

To quantify the rate of endocytosis of Ptc^{WT} and Ptc^{14} proteins, ectopic Ptc^{WT}GFP and Ptc^{14}GFP clones in the A compartment were induced and the endocytic compartment was labeled by incubation with Red-dextran (10 minute pulse). Using Metamorphic software, the PtcGFP fluorescence in the Red-dextran vesicles was measured and compared with the total PtcGFP signal in the clone. The resulting ratio was normalized to the Red-dextran vesicles in the clone cells. For this analysis, six confocal sections of seven different clones were measured and a total of 1459 vesicles for Ptc^{14} and 1650 for Ptc^{WT} were analyzed.

The content of HhGFP in the dotted pattern in wild-type and *ptc^{16}* mutant clones was also measured with Metamorph analysis software.

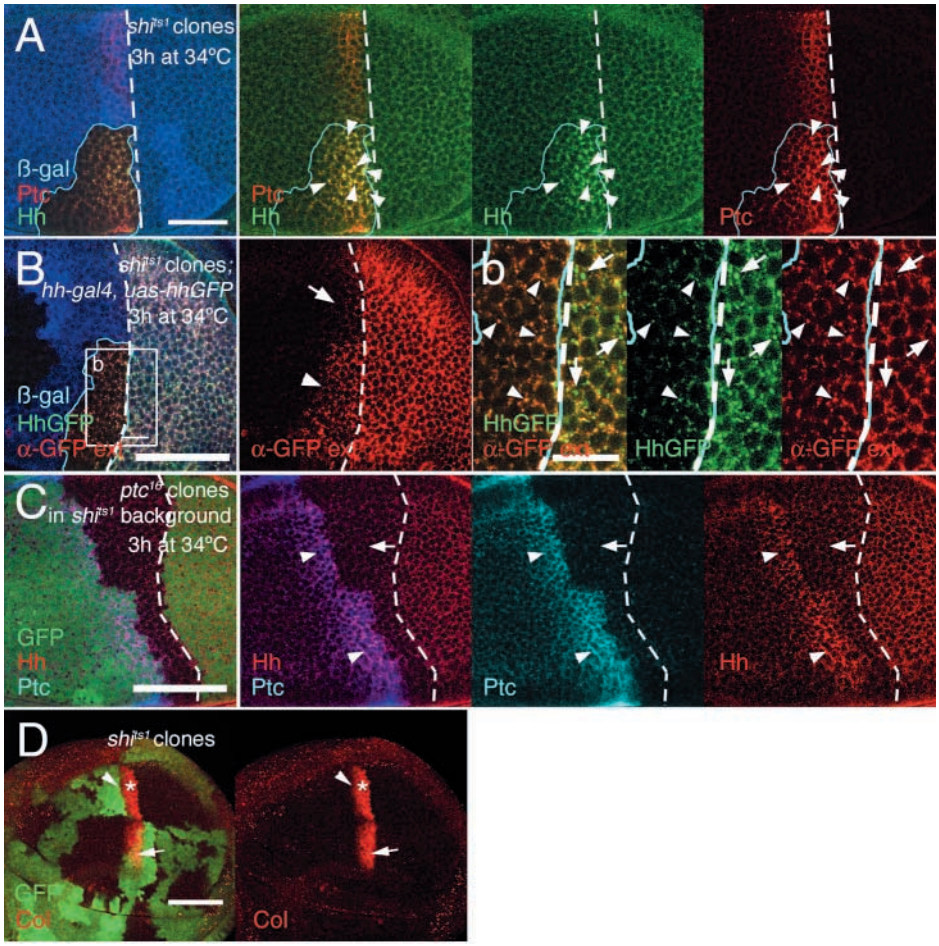

Fig. 3. Ptc is required for dynamin-dependent internalization of Hh. (A) *shi*^{ts1} A clone (labeled by the absence of β-Gal staining, blue) after 3 hours at the restrictive temperature that accumulates high levels of Hh (green) and Ptc (red) (arrowheads). (B) *shi*^{ts1} A clone after 3 hours at the restrictive temperature in a *hh-Gal4/UAS-HhGFP* wing disc. (b) Magnification of boxed area in B. The accumulation of Hh (green) in *shi*^{ts1} clone cells is extracellular, as shown by 'in vivo' incubation of the wing imaginal disc in a cold medium with anti-GFP antibody (red) (arrowheads, red panel in B and b). Note that the intracellular HhGFP (green and not red in the P compartment) is not labeled by this method (arrows in b). (C) *ptc*^{16} clone (labeled by absence of GFP, green) at the AP border in a *shi*^{ts1} wing disc after 3 hours at the restrictive temperature. Hh protein (red panel) does not accumulate in a *shi* background when Ptc protein is not present (blue panel) (arrow). Note that Hh crosses the Ptc^{-} territory and accumulates when it reaches the Ptc^{WT} area, just anterior to the clone (arrowheads). (D) *shi*^{ts1} clones (absence of GFP, green) in a wing imaginal disc after 10 hours at restrictive temperature. In *shi*^{ts1} clones there is not increase or decrease in Col expression after 10 hours at restrictive temperature (asterisk) compared with wild-type territory (arrow). There is not extension of signaling either (arrowhead). Scale bars: 50 μm in A-D; and 15 μm in b.

Each clone analyzed was compared with an equivalent region in the wild type territory of the same wing disc. The result from five different clones from independent experiments shows a ratio between 4 and 5 times more Hh in the wild-type cells.

Results

Patched controls the endocytosis of Hedgehog in a dynamin-dependent manner

In the wing imaginal disc epithelium, the A cells adjacent to the AP border express high levels of Ptc protein, the only known Hh receptor that mediates Hh endocytosis in *Drosophila* (Martín et al., 2001). To better analyze the Hh and Ptc interaction, we have used both HhGFP and PtcGFP tagged proteins in some of the experiments presented in this work. These fusion proteins behave as wild-type ones (for details, see Materials and methods, Figs 1, 2).

Here, we asked whether Hh internalization was required for the formation of the Hh gradient. In other signaling mechanisms, such as that of Dpp, the internalization of the morphogen is required for gradient formation (Entchev et al., 2000; Teleman and Cohen, 2000). To test this hypothesis, we used a thermo-sensitive *shibire* (*shi*) mutation. Shibire, the *Drosophila* Dynamin homolog, is needed for fission of clathrin-coated vesicles and the internalization of caveolae (van der Bliek, 1999). Shi mediates Ptc internalization in *Drosophila* embryos. In *shi*^{ts1} mutant embryos, a punctuate accumulation of Ptc at the plasma membrane was observed (Capdevila et al., 1994b), probably as a consequence of the accumulation of 'coated pits' at the plasma membrane (Kosaka and Ikeda, 1983). Here, we also observed a punctuate accumulation of both Ptc and Hh at cell surface in *shi*^{ts1} clones, close to the AP compartment border of the wing imaginal disc (Fig. 3A).

To test if the Hh accumulation was extracellular we used HhGFP fusion protein. *Hh-Gal4/HhGFP* third instar larvae containing *shi*^{ts1} clones were maintained at 32°C for 3 hours, a temperature that blocks Shi-dependent trafficking. Discs were then dissected and incubated with anti-GFP antibody in ice-cold medium prior to fixation. Under these experimental conditions, all trafficking processes were blocked and the antibody only labeled extracellular HhGFP molecules, while GFP fluorescence labeled both the intracellular and extracellular Hh. We noted that in the *shi* clone, all the green (HhGFP) fluorescence colocalized with the red (antibody-conjugated) fluorescence, indicating that all the retained Hh was extracellular (Fig. 3B,b, arrowheads).

Next, we addressed the question of whether Ptc might be responsible for the accumulation of Hh at the cell surface when endocytosis was blocked. To achieve this we made *ptc*^{16} clones (an amorphic allele, which does not produce Ptc protein, also known as *ptc*^{IIW109}) (Capdevila et al., 1994a) in a *shi*^{ts1} background. We found no build-up of Hh when Ptc

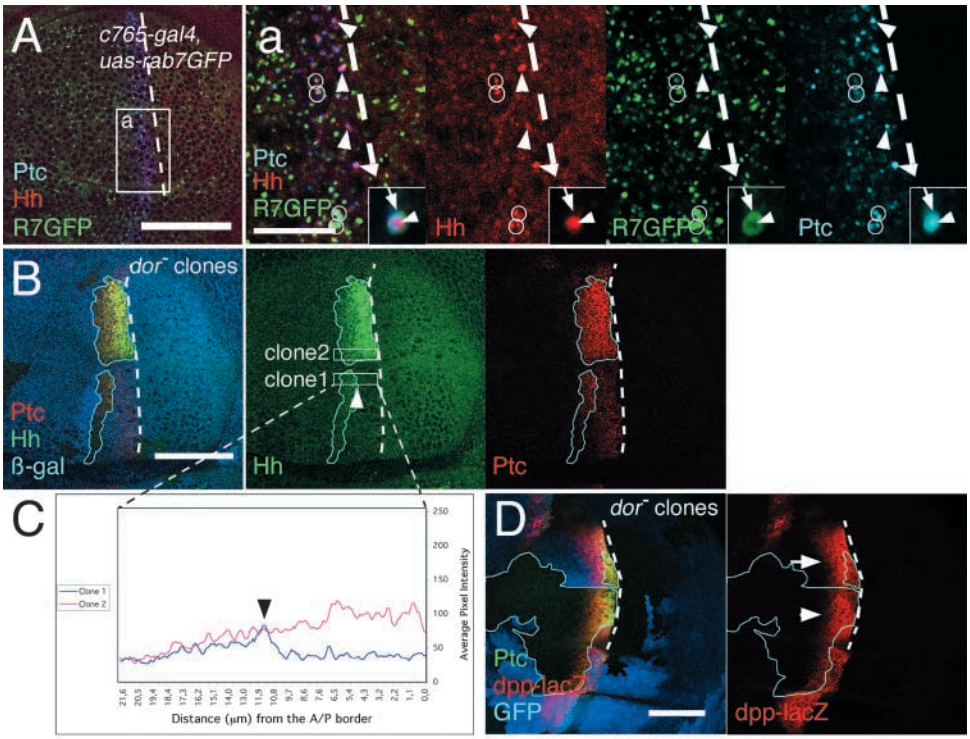

Fig. 4. Hh signaling is unaffected in *dor* mutant cells. (A) A confocal section of a *Rab-7GFP/c765-Gal4* wing imaginal disc, stained with anti-Ptc (blue) and anti-Hh (red) antibodies. (a) Magnification of boxed area in A. The staining shows co-localization of Hh, Ptc and Rab-7 at the AP compartment border (circles in a). There are also spots of Ptc and Hh colocalization that do not colocalize with Rab7 (arrowheads in a); these are probably early endosomes. The inset in a shows detail of the co-localization of the three proteins at some of these spots. Rab-7 shows doughnut-shaped GFP emission (arrow) surrounding the Ptc and Hh spots (arrowheads). (B) dor^{8} mutant clones (labeled by the lack of β-gal staining, blue) at the AP compartment border showing high accumulation of Hh (green) and Ptc (red) proteins because of the inhibition of lysosomal degradation. (C) Plot showing the green color pixel intensity of the cells in clone 1 (blue line) and clone 2 (red line) [corresponding to boxed areas in B (green panel)] with respect to the distance of the cells to the AP border. The same intensity (Hh accumulation) is seen in the A cells located at the same distance from the AP compartment border (arrowhead in B and C), whether Hh crosses (from the P compartment) a wild type (clone 1) or mutant (clone 2) area. (D) dor^{8} mutant clones (labeled by the lack of GFP staining, blue) close to the AP boundary showing no alteration in activation of the Hh targets [as shown by the expression of dpp-lacZ (red) (arrowhead) compared with its expression in the wild-type area (arrow)]. Scale bars: 50 μm in A,B,D; 15 μm in a.

protein was absent (Fig. 3C, red and blue panel, arrow), indicating that Shi-mediated Hh internalization was severely diminished in the absence of Ptc. We can therefore conclude that Ptc controls the endocytosis of Hh in a dynamin-dependent manner.

The accumulation of both Ptc and Hh at cell surface in shi^{ts1} clones, however, did not affect the activation of the Hh targets inside the clone (Fig. 3D, asterisk). Moreover, we did not observe an increase in the distance that Hh moves or signals in the anterior side of the shi^{ts1} clone (Fig. 3D, arrowhead). These observations suggest that although internalization of Hh is blocked in the shi^{ts1} mutants, Ptc has already sequestered Hh. This interpretation is in agreement with the blockage in Dynamin function at a stage where commitment to endocytic sequestration has already occurred (Kosaka and Ikeda, 1983; Ramaswami et al., 1994; Guha et al., 2003).

After internalization, Hh and Ptc are targeted to degradation

We previously reported that Ptc moves Hh to the endocytic compartment in the wing imaginal disc (Martín et al., 2001), after which degradation of Hh and Ptc would be expected. Rab-7 GTPase controls both protein trafficking to late endosomes and their subsequent fusion with lysosomes (reviewed by Zerial and McBride, 2001). A Rab-7GFP (Entchev et al., 2000) was used for labeling late endosomes. Ptc-Hh vesicles were found to colocalize with Rab-7GFP when this marker was expressed in all wing imaginal disc cells (Fig. 4A,a, circles). These results suggest that after internalization, Ptc and Hh go to late endosomes and lysosomes. Next, we examined whether the targeting of Hh to the degradative lysosomal pathway had any effect on Hh spreading and signaling. To block the degradative pathway, we used *deep orange* (*dor*) mutants, one of the mutations that affects eye pigmentation in *Drosophila* and is required for normal delivery of proteins to lysosomes (Sevrioukov et al., 1999). *dor* encodes the homolog of the yeast vacuole sorting protein Vps18p, a protein that as part of a complex regulates the function of Ypt7p, the paralog of Rab-7 in yeast (Rieder and Emr, 1997; Price et al., 2000). Blockage of the degradative pathway in dor^{-} mutant clones resulted in the accumulation of both Hh and Ptc (Fig. 4B). dor^{-} clones showed an Hh protein gradient in the A compartment of the wing imaginal disc (Fig. 4B), which was not observed when wild-type discs were stained with anti-Hh antibodies. As we have observed in shi^{ts1}, despite the large accumulation of Hh and Ptc in dor^{-} clones, the activation of Hh target genes remains unchanged, as shown by the normal *dpp-lacZ* (compare mutant territory in Fig. 4D, arrowhead, with wild-type territory, arrow) or *ptc-lacZ* expression (data not shown). These results indicate that both spreading and signaling are normal when Hh degradation is blocked in dor^{-} cells. Furthermore, the intensity of Hh immunofluorescence in the A cells located at the same distance from the AP border remains the same (Fig. 4B,C arrowheads), regardless of whether Hh had crossed wild-type (clone 1) or mutant (clone 2) territory. These data indicate that Ptc levels control the Hh gradient by sequestering Hh, and then both Hh and Ptc are targeted to degradation. They also

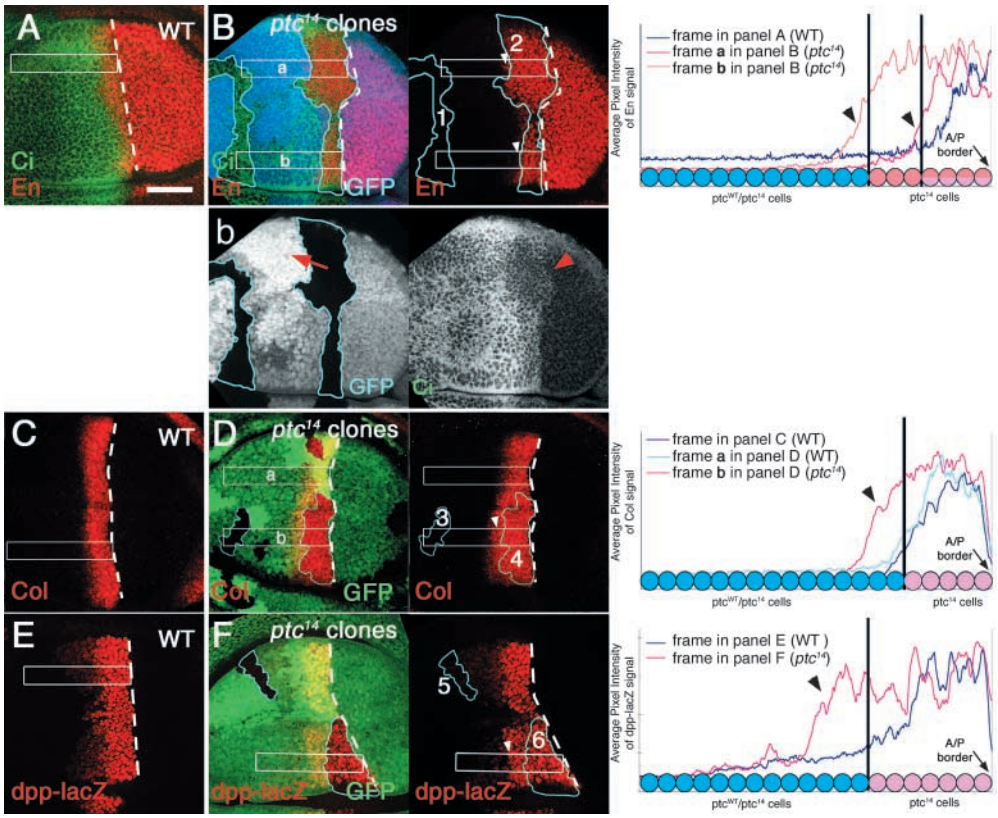

Fig. 5. Hh spreading is not impeded in *ptc*^{14} mutant clones but signaling is normal. (A,C,E) Wild-type expression of the Hh targets En (red) and Ci (green) (A), Col (red) (C) and Dpp (red) (E) in the third instar wing imaginal disc. (B,D,F) Activation of En, Col and Dpp (red) in *ptc*^{14} mutant clones abutting the AP compartment border (labeled by the lack of green GFP staining) (clones 2, 4 and 6) but not in clones outside the AP border (clones 1, 3 and 5). Note that Hh target gene activation occurs not only inside the clone touching the AP compartment border but also in cells located more anterior to the clone (arrowheads). The plots (right) show the fluorescence intensity for each target gene with respect to the distance of the cells to the AP border. The activation of the target genes occurs inside and anterior to the clone (arrowheads). Of 62 clones in the A compartment with A sister clones, 39 were located outside of the AP compartment border and did not show ectopic expression of En, Col and Dpp, and 23 were touching the compartment border showing activation of the targets inside and also in cells located anterior to the clone. (b) GFP signal and Ci staining of the disc in B. The clone touching the AP border has its twin in the A compartment (red arrow). The presence of the Ci staining sets the position of the AP border (red arrowhead). Scale bar: 50 μm.

suggest that Hh signaling is independent of Hh degradation by lysosomes.

Genetic uncoupling of the two Ptc functions

The analysis of Hh signaling in *shi* and *dor* mutant clones suggested that Hh sequestration and Hh signaling are independent. It has been proposed that Ptc regulates both signaling and sequestration (Chen and Struhl, 1996). This hypothesis was based on the analysis of the *ptc*^{S2} allele, which affects Hh signaling, but the sequestration of Hh is normal (Chen and Struhl, 1996; Martín et al., 2001; Strutt et al., 2001). The Ptc^{S2} mutant protein has a point mutation in the sterol-sensing domain (D584N) (Martín et al., 2001; Strutt et al., 2001) showing a preferential accumulation in endosomes (Martín et al., 2001).

As Ptc^{S2} is defective only in its signaling function, we used the *ptc*^{S2} allele to test for complementing alleles of *ptc* that might be defective for sequestration but not signaling. In this way, we identified the embryonic lethal *ptc*^{14} allele (also known as *ptc*^{IIR87}). Homozygous somatic *ptc*-null mutant clones induced in the A compartment produce the described *ptc*$^{-}$ mutant phenotype caused by the full activation of Hh targets (Phillips et al., 1990; Capdevila et al., 1994a; Tabata and Kornberg, 1994). By contrast, *ptc*^{14} mutant clones did not activate Hh signaling in the A compartment outside the AP border, as shown by the expression of Hh target genes such as *en*, *col*, *dpp*, *iro* or *ptc* itself (Fig. 5B-F clones 1, 3, 5; data not shown). Large clones (24-48 hours AEL) abutting the AP border activated En (Fig. 5B, clone 2), Col (Fig. 5D, clone 4) and *dpp* (Fig. 5F, clone 6) outside their normal expression domains. In addition to this activation, short-range, non-autonomous activation of En, Col and *dpp* extended a few cells outside the clone boundary (arrowheads in Fig. 5B,D,F). *ptc*^{14} cells therefore respond to maximum (En), medium (Col) and low [*dpp* (Fig. 5F) and Iro (data not shown)] levels of Hh, and Hh spreads throughout the clone and non-cautiously activates target genes a few cells outside the clone. To determine whether this effect was due to the presence of Hh, *ptc*^{14} clones were induced in an *hh*^{ts2} mutant background. After 30 hours at the restrictive temperature, *ptc*^{14} clones located neither outside nor close to the AP border activated Hh targets genes (Fig. 6B,D). These results indicate that Ptc^{14} activates the Hh pathway only in the presence of Hh, similar to wild-type Ptc. Furthermore, the broadened activation of target genes outside their normal expression domains in clones abutting the AP border indicates that *ptc*^{14} cells do not sequester Hh efficiently.

As *ptc*^{14} mutant clones extended the Hh gradient in the imaginal disc, we tested whether the embryonic phenotype depend on the presence of Hh. As in the imaginal disc, the *ptc*$^{-}$ embryonic phenotype is caused by a constitutive activation of the Hh pathway in cells that normally express Ptc (reviewed by Ingham and McMahon, 2001). It has been determined that *ptc* function is epistatic to *hh* function, because *ptc*$^{-}$*; hh*$^{-}$ double mutant embryos show the *ptc*$^{-}$ phenotype with the subsequent ectopic expression of Wg, as one of the Hh targets in the embryo (Ingham et al., 1991). *ptc*^{14} was originally

described as a null allele based on its embryonic phenotype (Nusslein-Volhard and Wieschaus, 1980) (Fig. 6E,F, middle panels). Nevertheless, the embryonic phenotype of the double mutant *ptc*^{14}*; hh*^{ts2} at the restrictive temperature (Fig. 6E, right panel) resembled that of *hh*$^{-}$ embryos, with no Wg expression (Fig. 6F, right panel). This indicates that the extended Wg expression observed in *ptc*^{14} mutant embryos was due to the presence of Hh, and not to the constitutive activation of the Hh pathway caused by the loss of *ptc* function.

Endocytosis defect in the Ptc^{14} mutant

The extended gradient of Hh across *ptc*^{14} mutant cells could be due to a defect in Ptc-Hh sequestration. The sequence of this allele confirmed a leucine to glutamic acid change (L83Q) at the first trans-membrane domain as previously reported (Strutt et al., 2001). To compare the ability of Ptc^{14} to sequester Hh with that of wild-type Ptc, both mutant and wild-type proteins were C-terminally tagged with GFP. Using these GFP tagged Ptc proteins we observed that the accumulation of Hh was much lower in Ptc^{14}GFP ectopic clones than in Ptc^{WT}GFP ectopic clones in the P compartment (compare Fig. 7A,a with 7B,b). This implies that Ptc^{14} sequesters Hh quite inefficiently.

Next, we analyzed the internalization of Hh and Ptc in *ptc*^{14} clones abutting at the AP compartment border. Fig. 7C shows a wing disc containing a *ptc*^{14} clone and its wild-type twin clone. The wild type AP border cells show the normal pattern of Hh and Ptc accumulation in endocytic vesicles (circles in Fig. 7c). In the *ptc*^{14} mutant clone, Ptc staining showed the same protein levels as in the wild-type territory (Fig. 7C, green panel). However, Ptc^{14} was not confined to punctuate structures, and Hh did not co-localize with Ptc^{14} (compare Fig. 7c and 7c′). This observation is in agreement with the lack of Hh sequestration observed in the ectopic Ptc^{14} mutant clones induced in the P compartment (Fig. 7B). To analyze this sequestration defect further, we made clones of *ptc*^{14} in a *shi*^{ts1} background and found that Hh was not accumulated at the plasma membrane inside the clone (Fig. 7D, asterisk) while in the Ptc wild-type cells anterior to the clone Hh was accumulated (Fig. 7D, arrowhead). This accumulation indicates that Hh can spread further through a ptc^{14} mutant territory than a wild-type territory. The behavior of Hh in these *shi*^{ts1}*; ptc*^{14} double mutant cells was similar to that observed in *ptc*^{16} clones (without Ptc protein) in a *shi*^{ts1} background (Fig. 3C). This result indicates that Ptc^{14} does not sequester Hh properly.

To explore a most likely failure in Ptc^{14}-mediated endocytosis of Hh, we examined the presence of Ptc^{14} compared with wild-type Ptc protein in endosomes. In wild-type cells, Ptc accumulates in early endocytic vesicles (Fig. 8A,a, circles), while in *ptc*^{14} cells Ptc^{14} does not accumulate in these structures (Fig. 8B,b, arrowheads). This lack of colocalization of Ptc^{14} with the endosomal marker could be due to the absence of Ptc^{14} at the plasma membrane. To test this possibility, discs expressing Ptc^{14}GFP ectopic clones were incubated ‘in vivo’ with an anti-Ptc antibody raised against the first extracellular loop of the Ptc protein (Capdevila et al., 1994b), in conditions of blocked trafficking processes (see Materials and methods). The extracellular labeling of Ptc in both Ptc^{WT}GFP (Fig. 8C) and Ptc^{14}GFP (Fig. 8D) ectopic clones indicates the presence of the mutant protein at the plasma membrane.

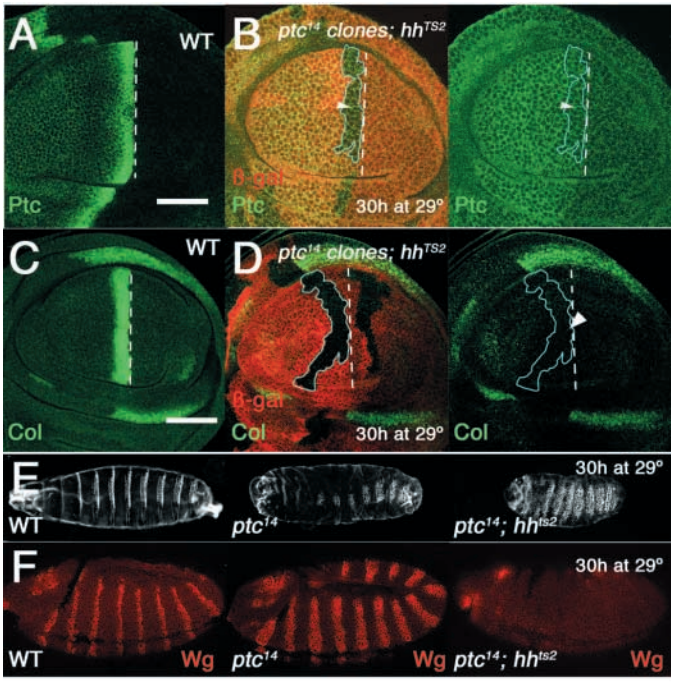

Fig. 6. Ptc^{14} activates the Hh pathway only in the absence of Hh. (A-D) The upregulation of Ptc (A) and Col (C) expression (green) at the AP compartment border observed in a wild-type wing disc is not produced in *ptc*^{14} clones (shown by the lack of β-gal staining, red) in an *hh*^{ts2} disc after 30 hours at the restrictive temperature (B,D; arrowheads). Of 20 clones in the A compartment with A sister clones, eight were touching the AP compartment border and did not showed activation of Ptc or Col at the restrictive temperature. (E) Cuticle preparation of wild-type, *ptc*^{14} and *ptc*^{14}*; hh*^{ts2} embryos at the restrictive temperature. Note that the double mutant *ptc*^{14}*; hh*^{ts2} embryo is like an *hh*$^{-}$ embryo, and not like a *ptc*$^{-}$ embryo, which would normally be the case with *ptc*$^{-}$*; hh*$^{-}$ double mutant embryos. (F) Wg expression pattern in wild-type, *ptc*^{14} and *ptc*^{14}*; hh*^{ts2} embryos at the restrictive temperature. In the *ptc*^{14} embryo, Wg stripes are broadened compared with the wild-type embryo, but Wg is not expressed in *ptc*^{14}*; hh*^{ts2} embryos at the restrictive temperature. Scale bars: 50 μm.

Having demonstrated that Ptc^{14} reaches the plasma membrane, we tested if the reduced ability of Ptc^{14} to internalize Hh was due to a defect of Ptc^{14} itself to enter the endocytic compartment. Thus, we examined the competence of ectopic Ptc^{WT}GFP and Ptc^{14}GFP to produce endocytic vesicles either in the presence or in the absence of Hh. In the absence of Hh, wild-type Ptc protein also accumulated in endosomes, as shown in Ptc^{WT}GFP ectopic clones located in areas of the A compartment that did not receive Hh (Fig. 8E,e, circles). This indicates that Ptc protein moves from the plasma membrane to the endocytic compartment in a ligand-independent manner, as has been shown in vertebrate cells (Incardona et al., 2002). However, Ptc^{14}GFP ectopic clones showed reduced amount of Ptc in endosomes, either in the presence (Fig. 8B,b, arrowheads) or absence of Hh (Fig. 8F,f, arrowheads). Therefore, we can conclude that Ptc^{14} cannot internalize Hh because of defective endocytosis by Ptc^{14}.

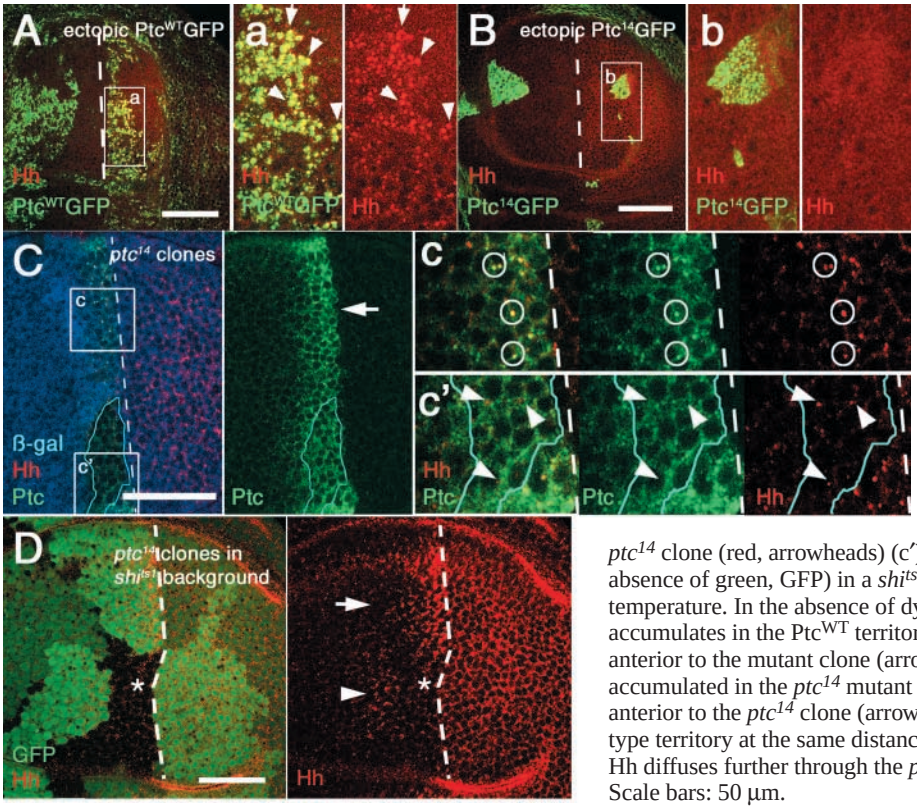

Fig. 7. Ptc^{14} does not internalize Hedgehog. (A,B) Ectopic wild type Ptc^{WT}GFP (A) and Ptc^{14}GFP (B) clones in the wing imaginal disc stained with anti-Hh antibody (red). (a,b) Detail of the clones shown in A and B. Only a few vesicles of Hh are observed in the clones expressing the Ptc^{14} mutant protein (Ptc^{14}GFP) (b) compared with those that express the wild-type Ptc protein (Ptc^{WT}GFP, arrows) (a). (C) Ptc (green) and Hh (red) expression in a wing imaginal disc containing a *ptc^{14}* clone (labeled by the absence of β-gal staining, blue). Ptc staining inside the clone (outlined in pale blue) has the same intensity levels than in the wild-type area (arrow, green panel). (c,c′) Magnification of the boxed areas in C. Ptc and Hh colocalize in spots in the wild-type area (circles) (c). Ptc does not accumulate in spots (green) in the *ptc^{14}* clone. However, Hh vesicles are still present in the *ptc^{14}* clone (red, arrowheads) (c′). (D) *ptc^{14}* clone at the AP border (shown by the absence of green, GFP) in a *shi^{ts1}* wing disc after 3 hours at the restrictive temperature. In the absence of dynamin-dependent internalization, Hh (red) accumulates in the Ptc^{WT} territories at the AP border and also in the Ptc^{WT} cells anterior to the mutant clone (arrowhead). However, Hh protein is not accumulated in the *ptc^{14}* mutant cells (asterisk). Note that the accumulation of Hh anterior to the *ptc^{14}* clone (arrowhead) is higher than the accumulation in wild-type territory at the same distance from the AP border (arrow). This indicates that Hh diffuses further through the *ptc^{14}* mutant cells than through wild-type cells. Scale bars: 50 μm.

The two functions of Ptc take place in different subcellular compartments

The complementation of *ptc^{14}*and *ptc^{S2}* alleles clearly indicates that Ptc has separate functions (one involved in signaling through an interaction with Smo and the other in Hh sequestration). But how Ptc performs both functions remains controversial. One can envision that if both proteins are localized in different subcellular compartments, indirect complementation might occur. Thus, while Ptc^{S2} is sequestering Hh in endosomes, Ptc^{14} could be interacting with Smo to control Hh signaling. Alternatively, both proteins Ptc^{S2} and Ptc^{14} might form a complex as part of the Ptc receptor, as previous studies have suggested (Johnson et al., 2000; Martín et al., 2001). To discriminate between these two possibilities, we used tagged versions of Ptc^{WT}GFP, Ptc^{S2}GFP and Ptc^{14}GFP to analyze the subcellular distribution of these mutant proteins in imaginal disc (data not shown) and salivary glands cells. Salivary glands cells are convenient for this experiments because are large and express endogenous Ptc protein at very low levels when Hh is not present (Zhu et al., 2003). In both systems, both Ptc^{WT}GFP and Ptc^{S2}GFP proteins were localized in large vesicles (Fig. 9A,B). However, Ptc^{14}GFP was found at the plasma membrane, consistent with the observations made in *ptc^{14}* mutant clones, and also in the membrane of the secretion vacuoles (Fig. 9C). Next, we examined the sub-cellular distribution of Ptc^{14}GFP protein when co-expressed with Ptc^{S2} (without GFP). Under these conditions, Ptc^{14}GFP was localized in vesicles resembling to Ptc^{WT}GFP localization (Fig. 9D). This change in the subcellular distribution of Ptc^{14}GFP strongly suggests that Ptc^{S2} and Ptc^{14} form a complex that re-establishes the wild-type function. Furthermore, these observations indicate that Hh signaling and sequestration take place in different subcellular compartments.

Is Hh still internalized in the absence of Ptc?

As Hh even signals normally in *ptc^{14}* mutant cells without Ptc mediated internalization, we went on to explore whether the mutant cells still internalized some Hh. So, we compared the internalization of Hh in either *ptc^{14}* clones or in clones of the null allele *ptc^{16}* induced at the AP compartment border in *Hh-Gal4/HhGFP* imaginal discs. In both cases, the same low amount of Hh was found in vesicles that did not co-localize with Ptc (Fig. 10A,a,C,c, arrowheads), but colocalize with internalized Red-dextran (Fig. 10B,b,D,d, circles). If Ptc were the only receptor for Hh, we would not expect to find Hh inside *ptc^{16}* cells, suggesting the presence of a Ptc-independent Hh internalization mechanism in the A compartment.

Discussion

We report genetic studies on Ptc function and its role in endocytosis during Hh signaling in *Drosophila*. We are able to show through the analysis of *ptc^{14}*, a mutant that does not internalize Hh but is able to perform Hh signal transduction, that both proposed Ptc functions are genetically uncoupled. We also show that Ptc limits the Hh gradient by internalizing Hh in a dynamin-dependent manner, and that this Hh-Ptc complex is targeted to the degradation pathway. These findings strongly suggest that internalization mediated by Ptc shapes the Hh gradient and also lead to the challenging suggestion that Hh signaling can occur in the absence of Ptc-mediated Hh

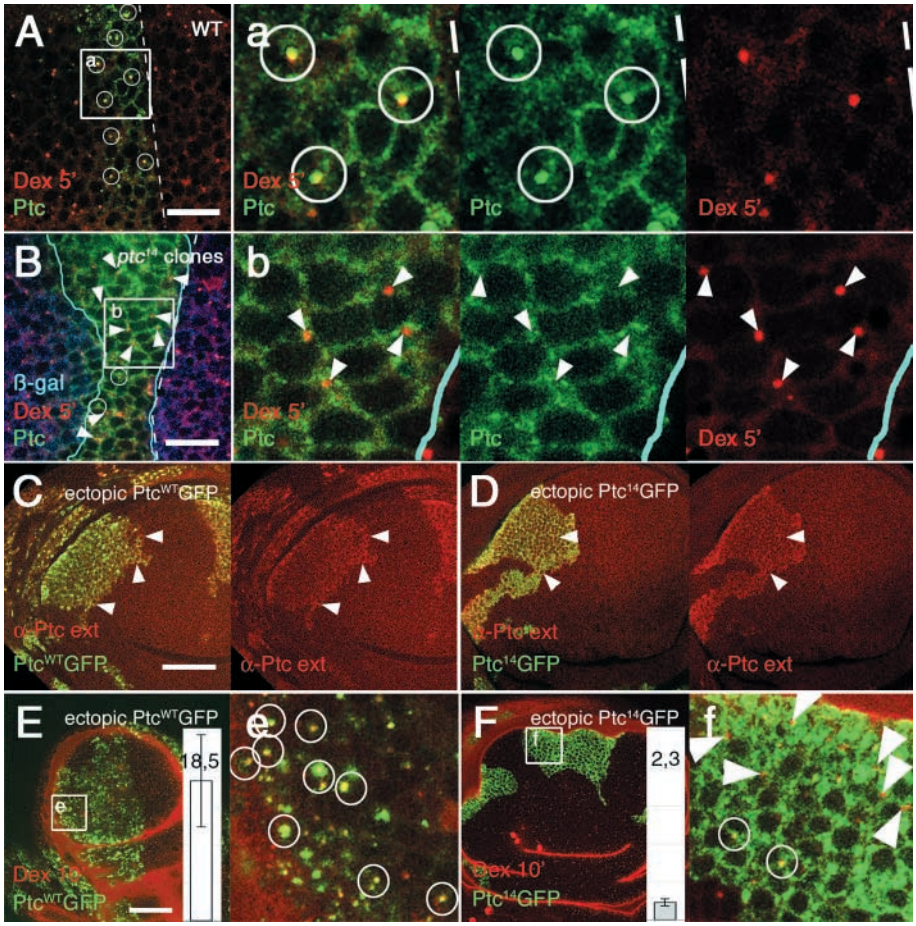

Fig. 8. Ptc^{14} does not accumulate in endosomes. (A,B) Internalized Red-dextran (5 minutes pulse) at the AP border of a wild-type wing imaginal disc (A) and in a *ptc^{14}* clone (B). (a) Details of the colocalization of Red-dextran positive vesicles and Ptc (green). (b) There is no colocalization of the internalized Red-dextran vesicles with Ptc protein in *ptc^{14}* clone cells. There is reduced Ptc staining in vesicles labeled with Red-dextran (green, arrowheads). Very few Red-dextran vesicles contain appreciable accumulation of Ptc (B, circles) compared with wild-type Ptc (A, circles). (C,D) Extracellular staining of Ptc in a wing disc containing ectopic Ptc^{WT}GFP (C) and Ptc^{14}GFP (D) clones using the anti-Ptc antibody, which recognizes one of the extracellular domains of Ptc. Staining is observed in both clones (arrowheads), indicating that a certain amount of Ptc^{WT}GFP and Ptc^{14}GFP reaches the plasma membrane. (E,F) Ptc^{WT}GFP (E) and Ptc^{14}GFP (F) ectopic clones in the A compartment far from the AP border in wing discs incubated with Red-dextran for 10 minutes. (e) Magnification of E showing the extensive co-localization between Ptc^{WT}GFP and internalized Red-dextran (circles), indicating that Ptc^{WT}GFP is endocytosed independently of the presence of Hh. (f) Magnification of F showing very little colocalization between Ptc^{14}GFP and internalized Red-dextran (arrowheads), indicating that Ptc^{14}GFP is not efficiently endocytosed. Circles indicate some Red-dextran vesicles with Ptc^{14}GFP accumulation. The analysis of the Ptc^{WT}GFP protein content in endocytic vesicles compared with the Ptc^{14}GFP mutant protein (E,F, columns) shows at least eight times more wild-type Ptc protein in endosomes than Ptc mutant protein (see Materials and methods). Scale bars: 15 μm in A,B; 50 μm in C-F.

internalization. We will now discuss the two functions of Ptc in Hh signal transduction in the light of our results.

Role of Ptc in Hh gradient formation

We have shown here that Hh and Ptc sorting to the endocytic membrane-bound compartment plays a crucial role in modulating Hh levels during development. A strong support of the conclusions in this work comes from the analysis of the *ptc^{14}* allele. Although *ptc^{14}* mutants are lethal with a strong *ptc^{-}* embryonic phenotype, *ptc^{14}* mutant cells in the imaginal discs showed an effect only when the clone touched the AP compartment border but not in any other part of the disc. This result indicates that the presence of Hh is required to reveal a defect in Ptc^{14} function. This Hh requirement has been probed by the no activation of the Hh targets in *ptc^{14}* cells in the absence of Hh either in the embryos or in the imaginal discs. The complementation of *ptc^{14}* with *ptc^{S2}* allele, which is considered as null for blocking Hh signal transduction and acts as dominant negative (Martín et al., 2001; Strutt et al., 2001), indicates that Ptc^{14} does not have a greater sensibility to Hh than the Ptc wild-type protein. Conversely, it is shown here that there is a decrease of internalization of Hh in *ptc^{14}* mutant clones compared with wild-type Ptc territory and an extension of the range of Hh gradient. Therefore, we can conclude that Ptc^{14} is unable to sequester Hh efficiently in either the embryo or imaginal discs and that the *ptc^{14}* embryonic phenotype would be the result of greater spreading of Hh and not to the constitutive activation of the Hh pathway.

Ptc^{14} responds to Hh as the wild-type Ptc protein and activates the signaling pathway indicating that the interaction of Ptc^{14} and Hh is probably normal. However, this Hh-Ptc interaction does not necessarily imply sequestration. Although Ptc^{14} occurs at the plasma membrane, we do not observe internalization of Hh or extracellular Hh accumulation in *ptc^{14}* mutant clones. These results, therefore, suggest that Hh-Ptc interaction is not sufficient to sequester Hh and that an active internalization process of Hh mediated by Ptc to control Hh gradient is required. This Hh internalization mediated by Ptc is Dynamin-dependent, based on the membrane accumulation of Hh and Ptc in *shi* mutant clones and the lack of accumulation of Hh in *shi^{ts1}; ptc^{16}* double mutant clones. However, the initiation of the internalization process is not blocked in *shi* mutants because Dynamin is required for fission of clathrin-coated vesicles after the internalization process has already started (Kosaka and Ikeda, 1983; Ramaswami et al., 1994; Guha et al., 2003). This fact would explain why Hh gradient and signaling is not extended when endocytosis is blocked in *shi* mutant cells. As Ptc^{14} seems to have a problem in entering the endocytic compartment and we

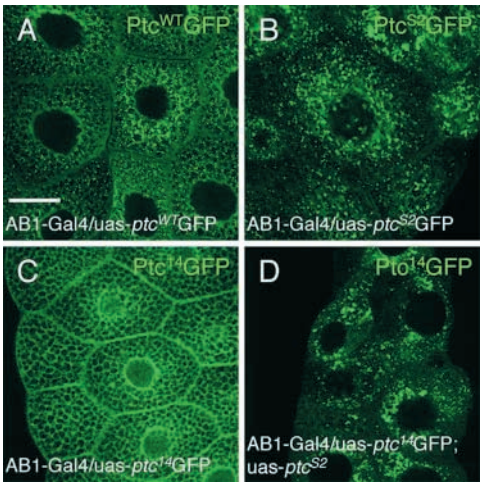

Fig. 9. Co-expression of Ptc^{S2} and Ptc^{14} recovers the normal subcellular distribution of Ptc^{14} protein. (A-C) The distinct staining patterns of Ptc^{WT}GFP (A), Ptc^{S2}GFP (B) and Ptc^{14}GFP (C) in salivary glands cells (using the *AB1-Gal4* driver). (D) The subcellular distribution of Ptc^{14}GFP protein in salivary gland cells changes to the wild-type pattern when it is co-expressed with non-labeled Ptc^{S2}. Scale bar: 30 μm.

have not found Hh accumulation in shi^{ts1}; ptc^{14} double mutant clones we conclude that the initiation of the internalization process does not occur in Ptc^{14}. Taken together, these data indicate that only when Ptc forces Hh to the endocytic pathway Hh is sequestered in the receiving cells.

The behavior of Hh and Ptc in dor^{-} cells indicates that after sequestration, Ptc internalizes Hh, and both Hh and Ptc are degraded. Thus, controlling both endocytosis and degradation of Hh modulates its gradient. Similar mechanisms have been described for controlling the asymmetric gradient of Wg in embryonic segments (Dubois et al., 2001). It is possible that additional factors may contribute to shaping the Hh gradient, because in large ptc^{-} clones close to the AP border, which lack Ptc protein to sequester Hh, an Hh gradient in endocytic vesicles was also observed, although the range of this gradient was more extended than in wild-type cells (data not shown). This is consistent with two mechanisms of Hh internalization in Hh receiving cells as we have observed, one mediated by Ptc and another not mediated by Ptc.

Role of Ptc in Hh signal transduction

From studies in both vertebrates and *Drosophila*, it was thought that Hh protein binds to Ptc (Stone et al., 1996; Fuse et al., 1999). Ptc is then internalized and traffics Hh to endosomal compartments where both are degraded (Denef et al., 2000; Incardona et al., 2002), the entire process triggering activation of the Hh pathway. It is shown here that Ptc^{14} responds to Hh as would the wild-type Ptc protein in activating the pathway.

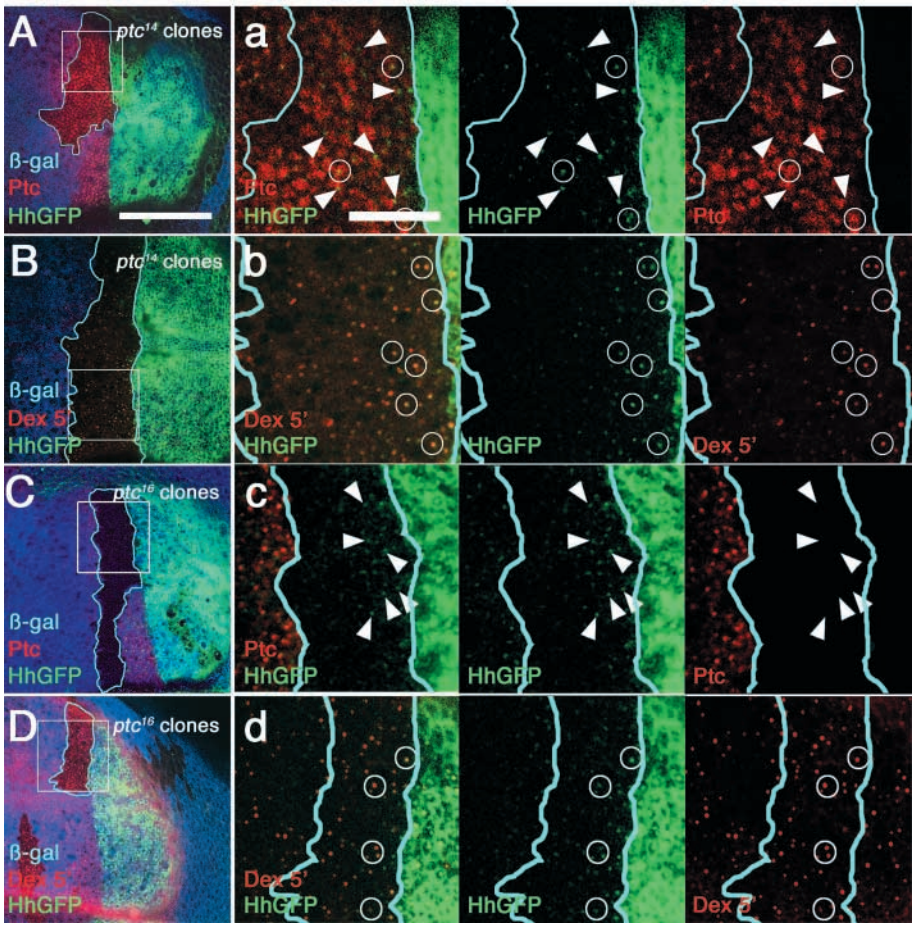

Fig. 10. Hh internalization in Hh-receiving cells in the absence of Ptc. (A) ptc^{14} clone (labeled by the lack of β-gal staining, blue) abutting the AP compartment border in an *hh-Gal4/UAS-HhGFP* background stained with anti-Ptc antibody (red). (a) Magnification of the same ptc^{14} clone in A. There is no colocalization between HhGFP punctuate structures and Ptc^{14} (arrowheads). Only a few of the Hh-GFP vesicles show colocalization with Ptc staining, though not as spots (circles). Compare with HhGFP staining in a wild-type background (Fig. 1D). (B) ptc^{14} clone in an *hh-Gal4/UAS-HhGFP* wing disc with internalized Red-dextran. (b) Magnification of the ptc^{14} clone in B. HhGFP vesicles do not colocalize with Ptc but most of them colocalize with internalized Red-dextran (circles). (C) ptc^{16} clone (indicated by the lack of β-gal staining, blue) abutting the AP compartment border in an *hh-Gal4/UAS-HhGFP* background stained with anti-Ptc antibody (red). (c) Magnification of the ptc^{16} clone in C. (D) ptc^{16} clone in an *hh-Gal4/UAS-HhGFP* wing disc showing the internalized Red-dextran. (d) Magnification of the ptc^{16} clone in D. Observe the HhGFP punctuate structures (green, arrowheads) in A cells close to the AP border with no Ptc protein (c). These structures colocalize with Red-dextran (circles; d). Scale bars: 50 μm in A-D; 15 μm in a-d.

However, Ptc^{14} does not internalize Hh to the endocytic compartment because is defective in endocytosis. We therefore suggest that the massive Hh internalization by Ptc to control the gradient is not a requirement for Hh pathway signal transduction.

In Hh signal transduction, the cellular mechanisms that regulate Smo function remain unclear, although the distribution of Ptc/Smo suggests that Ptc destabilizes Smo levels (Alcedo et al., 2000; Denef et al., 2000; Ingham et al., 2000). It has also been proposed that Ptc-mediated Hh internalization changes the subcellular localization of Ptc preventing Smo downregulation (Denef et al., 2000). Furthermore, in cultured cells, Shh induces the segregation of Ptc and Smo in endosomes, allowing Smo signaling, independently of Ptc (Incardona et al., 2002). It is known, however, that binding of Shh to Ptc is not sufficient to relieve the repression of the Hh pathway (Williams et al., 1999).

We show that as in wild-type cells, in the absence of Hh, Ptc^{14} downregulates both Smo levels and Smo activity, while in the presence of Hh, the normal upregulation of Smo occurs. Consequently, Ptc^{14} levels are high at the AP border because upregulation of Ptc by Hh occurs in the absence of internalization of Hh to the degradative pathway. It might then be expected that the high levels of Ptc^{14} not targeted to the degradative pathway would block Smo activity. However, against all predictions, the presence of Hh is still able to release Smo activity in mutant *ptc^{14}* cells. Thus, there must be a positive mediator of Smo activity to overcome the repressive effect of Ptc^{14} and allow Hh pathway activation in response to Hh. Alternatively, if Ptc^{14} is located at the plasma membrane, it could control Smo activity without entering the endocytic compartment by regulating the entrance of small molecules, as has been recently proposed (Taipale et al., 2002). In fact, Ptc is similar to a family of bacterial proton-gradient-driven transmembrane molecule transporters known as RND proteins (Tseng et al., 1999). Accordingly, as a membrane transporter, Ptc could indirectly inhibit Smo through translocation of a small molecule that conformationally regulates the active state of Smo (Tseng et al., 1999). The inter-allelic complementation of Ptc suggests that Ptc has the oligomeric structure needed for this type of transporter.

Although one of the normal functions of Ptc is to mediate Hh internalization, the data demonstrate the presence of internalized Hh vesicles in the absence of Ptc protein. It is therefore suggested that another receptor mediates Hh internalization in Hh-receiving cells. This molecule could act as a positive mediator of Hh signaling. Several observations have been published that cannot easily be reconciled with the idea of Ptc acting as the only receptor for Hh. For example, it was found that Hh activates signal transduction in both A and P compartment cells of wing imaginal discs, despite the absence of Ptc in P cells (Ramirez-Weber et al., 2000; Amanai and Jiang, 2001). Furthermore, it has been reported that some neuroblasts in *Drosophila* embryos, the maturation of which is dependent on Hh, do not express or require Ptc (Bhat and Schedl, 1997). This suggests that a receptor other than Ptc mediates Hh signaling. Recently, the glypican protein Dally-like, which belongs to the heparan sulfate proteoglycan protein family, was found to be required for Hh signal transduction and probably for the reception of the Hh signal in *Drosophila* tissue culture cells (Desbordes and Sanson, 2003; Lum et al., 2003). Dally-like could act as co-receptor for Hh and it would be interesting to know if Dally-like is required for Hh endocytosis. In addition, the large glycoprotein 'Megalin' has recently been identified as Shh-binding protein (McCarthy et al., 2002). Megalin is a multi-ligand-binding protein of the low-density lipoprotein (LDL) receptor family whose function is to mediate the endocytosis of ligands (Argraves, 2001) (reviewed by Christensen and Birn, 2002). The finding that megalin-mediated endocytosed N-Shh was not efficiently targeted to lysosomes for degradation suggests that N-Shh may also traffic in complexes with Megalin and thus be recycled and/or transcytosed (Argraves, 2001). In the Wg pathway, specific LDL receptor-related proteins are essential co-receptors for Wnt ligands (Wehrli et al., 2000). Further investigation will determine whether LDL receptor-related proteins could function as co-receptors that internalize Hh in the absence of Ptc. Alternatively, these proteins could be required for endocytosis and further delivery of Hh to Ptc in intracellular vesicles, perhaps facilitating the transcytosis of Hh. A future challenge will be to find other molecules that internalize Hh and to understand how Hh interacts with Smo to activate the Hh pathway.

We are grateful to Ignacio Sandoval for his advice and discussion during the work process, and also for his comments on the manuscript. We are also very grateful to Carmen Ibáñez for her excellent technical assistance. We thank Alfredo Villasante, David Gubb and Tom Kornberg for their comments on the manuscript. We also thank S. Cohen for the anti-Smo antibody, A. Vincent for the anti-Col antibody, R. Holmgren for the anti-Ci antibody, T. Kornberg for the anti-Hh antibody, and F. De Celis, M. González-Gaitán, H. Krämer, G. Struhl, T. Tabata and S. L. Zipurski for fly strains. This work was financed by the Spanish MCYT grant BMC2002-03839, the Comunidad Autónoma de Madrid grant 08.6/0045/2001.2, and by an institutional grant from the Fundación Areces. C.T. was financially supported by fellowships awarded by the Comunidad Autónoma de Madrid, and N.G. by an I3P fellowship awarded by the CSIC.

References

Alcedo, J., Zou, Y. and Noll, M. (2000). Posttranscriptional regulation of smoothened is part of a self-correcting mechanism in the Hedgehog signaling system. *Mol. Cell* **6**, 457-465.

Amanai, K. and Jiang, J. (2001). Distinct roles of Central missing and Dispatched in sending the Hedgehog signal. *Development* **128**, 5119-5127.

Argraves, W. S. (2001). Members of the low density lipoprotein receptor family control diverse physiological processes. *Front. Biosci.* **6**, D406-D416.

Basler, K. and Struhl, G. (1994). Compartment boundaries and the control of Drosophila limb pattern by hedgehog protein. *Nature* **368**, 208-214.

Bhat, K. M. and Schedl, P. (1997). Requirement for engrailed and invected genes reveals novel regulatory interactions between engrailed/invected, patched, gooseberry and wingless during Drosophila neurogenesis. *Development* **124**, 1675-1688.

Blackman, R. K., Sanicola, M., Raftery, L. A., Gillevet, T. and Gelbart, W. M. (1991). An extensive 3′ cis-regulatory region directs the imaginal disk expression of decapentaplegic, a member of the TGF-beta family in Drosophila. *Development* **111**, 657-666.

Brand, A. H. and Perrimon, N. (1993). Targeted gene expression as a means of altering cell fates and generating dominant phenotypes. *Development* **118**, 401-415.

Brook, W. J. and Cohen, S. M. (1996). Antagonistic interactions between wingless and decapentaplegic responsible for dorsal-ventral pattern in the Drosophila Leg. *Science* **273**, 1373-1377.

Burke, R., Nellen, D., Bellotto, M., Hafen, E., Senti, K. A., Dickson, B. J. and Basler, K. (1999). Dispatched, a novel sterol-sensing domain protein

dedicated to the release of cholesterol-modified hedgehog from signaling cells. *Cell* **99**, 803-815.

Capdevila, J., Estrada, M. P., Sanchez-Herrero, E. and Guerrero, I. (1994a). The Drosophila segment polarity gene patched interacts with decapentaplegic in wing development. *EMBO J.* **13**, 71-82.

Capdevila, J., Pariente, F., Sampedro, J., Alonso, J. L. and Guerrero, I. (1994b). Subcellular localization of the segment polarity protein patched suggests an interaction with the wingless reception complex in Drosophila embryos. *Development* **120**, 987-998.

Chen, Y. and Struhl, G. (1996). Dual roles for patched in sequestering and transducing Hedgehog. *Cell* **87**, 553-563.

Christensen, E. I. and Birn, H. (2002). Megalin and cubilin: multifunctional endocytic receptors. *Nat. Rev. Mol. Cell Biol.* **3**, 256-266.

de Celis, J. F. and Bray, S. (1997). Feed-back mechanisms affecting Notch activation at the dorsoventral boundary in the *Drosophila* wing. *Development* **124**, 3241-3251.

Denef, N., Neubuser, D., Perez, L. and Cohen, S. M. (2000). Hedgehog induces opposite changes in turnover and subcellular localization of patched and smoothened. *Cell* **102**, 521-531.

Desbordes, S. C. and Sanson, B. (2003). The glypican Dally-like is required for Hedgehog signalling in the embryonic epidermis of Drosophila. *Development* **130**, 6245-6255.

Diez del Corral, R., Aroca, P., Gómez-Skarmeta, J., Cavodeassi, F. and Modolell, J. (1999). The Iroquois homeodomain proteins are required to specify body wall identity in Drosophila. *Genes Dev.* **13**, 1754-1761.

Dubois, L., Lecourtois, M., Alexandre, C., Hirst, E. and Vincent, J. P. (2001). Regulated endocytic routing modulates wingless signaling in Drosophila embryos. *Cell* **105**, 613-624.

Eldar, A., Rosin, D., Shilo, B. Z. and Barkai, N. (2003). Self-enhanced ligand degradation underlies robustness of morphogen gradients. *Dev. Cell* **5**, 635-646.

Entchev, E. V., Schwabedissen, A. and Gonzalez-Gaitan, M. (2000). Gradient formation of the TGF-beta homolog Dpp. *Cell* **103**, 981-991.

Fuse, N., Maiti, T., Wang, B., Porter, J. A., Hall, T. M., Leahy, D. J. and Beachy, P. A. (1999). Sonic hedgehog protein signals not as a hydrolytic enzyme but as an apparent ligand for patched. *Proc. Natl. Acad. Sci. USA* **96**, 10992-10999.

García-Bellido, A., Ripoll, P. and Morata, G. (1973). Developmental compartmentalisation of the wing disk of Drosophila. *Nat. New Biol.* **245**, 251-253.

Greco, V., Hannus, M. and Eaton, S. (2001). Argosomes. A potential vehicle for the spread of morphogens through epithelia. *Cell* **106**, 633-645.

Grigliatti, T. A., Hall, L., Rosenbluth, R. and Suzuki, D. T. (1973). Temperature-sensitive mutations in Drosophila melanogaster. XIV. A selection of immobile adults. *Mol. Gen. Genet.* **120**, 107-114.

Guha, A., Sriram, V., Krishnan, K. S. and Mayor, S. (2003). Shibire mutations reveal distinct dynamin-independent and -dependent endocytic pathways in primary cultures of Drosophila hemocytes. *J. Cell Sci.* **116**, 3373-3386.

Incardona, J. P., Gruenberg, J. and Roelink, H. (2002). Sonic hedgehog induces the segregation of patched and smoothened in endosomes. *Curr. Biol.* **12**, 983-995.

Ingham, P. W. and McMahon, A. P. (2001). Hedgehog signaling in animal development: paradigms and principles. *Genes Dev.* **15**, 3059-3087.

Ingham, P. W., Taylor, A. M. and Nakano, Y. (1991). Role of the Drosophila patched gene in positional signalling. *Nature* **353**, 184-187.

Ingham, P. W., Nystedt, S., Nakano, Y., Brown, W., Stark, D., van den Heuvel, M. and Taylor, A. M. (2000). Patched represses the Hedgehog signalling pathway by promoting modification of the Smoothened protein. *Curr. Biol.* **10**, 1315-1318.

Johnson, R. L., Grenier, J. K. and Scott, M. P. (1995). patched overexpression alters wing disc size and pattern: transcriptional and post-transcriptional effects on hedgehog targets. *Development* **121**, 4161-4170.

Johnson, R. L., Milenkovic, L. and Scott, M. P. (2000). In vivo functions of the patched protein: requirement of the C terminus for target gene inactivation but not Hedgehog sequestration. *Mol. Cell* **6**, 467-478.

Kosaka, T. and Ikeda, K. (1983). Reversible blockage of membrane retrieval and endocytosis in the garland cell of the temperature-sensitive mutant of Drosophila melanogaster, shibirets1. *J. Cell Biol.* **97**, 499-507.

Kuwabara, P. E. and Labouesse, M. (2002). The sterol-sensing domain: multiple families, a unique role? *Trends Genet.* **18**, 193-201.

Lander, A. D., Nie, Q. and Wan, F. Y. (2002). Do morphogen gradients arise by diffusion? *Dev. Cell* **2**, 785-796.

Lecuit, T. and Cohen, S. M. (1998). Dpp receptor levels contribute to shaping the Dpp morphogen gradient in the Drosophila wing imaginal disc. *Development* **125**, 4901-4907.

Lee, J. J., Ekker, S. C., von, K. D., Porter, J. A., Sun, B. I. and Beachy, P. A. (1994). Autoproteolysis in hedgehog protein biogenesis [see comments]. *Science* **266**, 1528-1537.

Lum, L., Yao, S., Mozer, B., Rovescalli, A., von Kessler, D., Nirenberg, M. and Beachy, P. A. (2003). Identification of Hedgehog pathway components by RNAi in Drosophila cultured cells. *Science* **299**, 2039-2045.

Ma, C., Zhou, Y., Beachy, P. A. and Moses, K. (1993). The segment polarity gene hedgehog is required for progression of the morphogenetic furrow in the developing Drosophila eye. *Cell* **75**, 927-938.

Martín, V., Carrillo, G., Torroja, C. and Guerrero, I. (2001). The sterol-sensing domain of Patched protein seems to control Smoothened activity through Patched vesicular trafficking. *Curr. Biol.* **11**, 601-607.

McCarthy, R. A., Barth, J. L., Chintalapudi, M. R., Knaak, C. and Argraves, W. S. (2002). Megalin functions as an endocytic sonic hedgehog receptor. *J. Biol. Chem.* **277**, 25660-25667.

Motzny, C. K. and Holmgren, R. (1995). The Drosophila cubitus interruptus protein and its role in the wingless and hedgehog signal transduction pathways. *Mech. Dev.* **52**, 137-150.

Munro, S. and Freeman, M. (2000). The notch signalling regulator fringe acts in the Golgi apparatus and requires the glycosyltransferase signature motif DXD. *Curr. Biol.* **10**, 813-820.

Nellen, D., Burke, R., Struhl, G. and Basler, K. (1996). Direct and long-range action of a DPP morphogen gradient. *Cell* **85**, 357-368.

Nusslein-Volhard, C. and Wieschaus, E. (1980). Mutations affecting segment number and polarity in Drosophila. *Nature* **287**, 795-801.

Patel, N. H., Martin, B. E., Coleman, K. G., Poole, S. J., Ellis, M. C., Kornberg, T. B. and Goodman, C. S. (1989). Expression of engrailed proteins in arthropods, annelids, and chordates. *Cell* **58**, 955-968.

Pepinsky, R. B., Rayhorn, P., Day, E. S., Dergay, A., Williams, K. P., Galdes, A., Taylor, F. R., Boriack-Sjodin, P. A. and Garber, E. A. (2000). Mapping sonic hedgehog-receptor interactions by steric interference. *J. Biol. Chem.* **275**, 10995-11001.

Phillips, R. G., Roberts, I. J., Ingham, P. W. and Whittle, J. R. (1990). The Drosophila segment polarity gene patched is involved in a position-signalling mechanism in imaginal discs. *Development* **110**, 105-114.

Pignoni, F. and Zipursky, S. L. (1997). Induction of Drosophila eye development by decapentaplegic. *Development* **124**, 271-278.

Porter, J. A., von, K. D., Ekker, S. C., Young, K. E., Lee, J. J., Moses, K. and Beachy, P. A. (1995). The product of hedgehog autoproteolytic cleavage active in local and long-range signalling. *Nature* **374**, 363-366.

Price, A., Seals, D., Wickner, W. and Ungermann, C. (2000). The docking stage of yeast vacuole fusion requires the transfer of proteins from a cis-SNARE complex to a Rab/Ypt protein. *J. Cell Biol.* **148**, 1231-1238.

Ramaswami, M., Krishnan, K. S. and Kelly, R. B. (1994). Intermediates in synaptic vesicle recycling revealed by optical imaging of Drosophila neuromuscular junctions. *Neuron* **13**, 363-375.

Ramirez-Weber, F. A., Casso, D. J., Aza-Blanc, P., Tabata, T., Kornberg, T. B., Lin, H., Ruiz, I. A. A., Alcedo, J., Zou, Y. and Noll, M. (2000). Hedgehog signal transduction in the posterior compartment of the *Drosophila* wing imaginal disc. *Mol. Cell* **6**, 479-485.

Rieder, S. E. and Emr, S. D. (1997). A novel RING finger protein complex essential for a late step in protein transport to the yeast vacuole. *Mol. Biol. Cell* **8**, 2307-2327.

Royet, J. and Finkelstein, R. (1997). Establishing primordia in the Drosophila eye-antennal imaginal disc: the roles of decapentaplegic, wingless and hedgehog. *Development* **124**, 4793-4800.

Sánchez-Herrero, E., Couso, J. P., Capdevila, J. and Guerrero, I. (1996). The fu gene discriminates between pathways to control dpp expression in Drosophila imaginal discs. *Mech. Dev.* **55**, 159-170.

Seto, E. S., Bellen, H. J. and Lloyd, T. E. (2002). When cell biology meets development: endocytic regulation of signaling pathways. *Genes Dev.* **16**, 1314-1336.

Sevrioukov, E. A., He, J. P., Moghrabi, N., Sunio, A. and Kramer, H. (1999). A role for the deep orange and carnation eye color genes in lysosomal delivery in Drosophila. *Mol. Cell* **4**, 479-486.

Shestopal, S. A., Makunin, I. V., Belyaeva, E. S., Ashburner, M. and Zhimulev, I. F. (1997). Molecular characterization of the deep orange (dor) gene of Drosophila melanogaster. *Mol. Gen. Genet.* **253**, 642-648.

Stone, D. M., Hynes, M., Armanini, M., Swanson, T. A., Gu, Q., Johnson, R. L., Scott, M. P., Pennica, D., Goddard, A., Phillips, H. et al. (1996).

The tumour-suppressor gene patched encodes a candidate receptor for Sonic hedgehog. *Nature* **384**, 129-134.

Strigini, M. and Cohen, S. M. (2000). Wingless gradient formation in the Drosophila wing. *Curr. Biol.* **10**, 293-300.

Strutt, H., Thomas, C., Nakano, Y., Stark, D., Neave, B., Taylor, A. M. and Ingham, P. W. (2001). Mutations in the sterol-sensing domain of Patched suggest a role for vesicular trafficking in Smoothened regulation. *Curr. Biol.* **11**, 608-613.

Tabata, T. and Kornberg, T. B. (1994). Hedgehog is a signaling protein with a key role in patterning Drosophila imaginal discs. *Cell* **76**, 89-102.

Taipale, J., Cooper, M. K., Maiti, T. and Beachy, P. A. (2002). Patched acts catalytically to suppress the activity of Smoothened. *Nature* **418**, 892-897.

Teleman, A. A. and Cohen, S. M. (2000). Dpp gradient formation in the Drosophila wing imaginal disc. *Cell* **103**, 971-980.

Tseng, T. T., Gratwick, K. S., Kollman, J., Park, D., Nies, D. H., Goffeau, A. and Saier, M. H., Jr (1999). The RND permease superfamily: an ancient, ubiquitous and diverse family that includes human disease and development proteins. *J. Mol. Microbiol. Biotechnol.* **1**, 107-125.

van der Bliek, A. M. (1999). Functional diversity in the dynamin family. *Trends Cell Biol.* **9**, 96-102.

Vervoort, M., Crozatier, M., Valle, D. and Vincent, A. (1999). The COE transcription factor collier is a mediator of short-range hedgehog-induced patterning of the drosophila wing. *Curr. Biol.* **9**, 632-639.

Vincent, J. P. and Dubois, L. (2002). Morphogen transport along epithelia, an integrated trafficking problem. *Dev. Cell* **3**, 615-623.

Wehrli, M., Dougan, S. T., Caldwell, K., O'Keefe, L., Schwartz, S., Vaizel-Ohayon, D., Schejter, E., Tomlinson, A. and DiNardo, S. (2000). arrow encodes an LDL-receptor-related protein essential for Wingless signalling. *Nature* **407**, 527-530.

Williams, K. P., Rayhorn, P., Chi-Rosso, G., Garber, E. A., Strauch, K. L., Horan, G. S., Reilly, J. O., Baker, D. P., Taylor, F. R., Koteliansky, V. et al. (1999). Functional antagonists of sonic hedgehog reveal the importance of the N terminus for activity. *J. Cell Sci.* **112**, 4405-4414.

Zecca, M., Basler, K. and Struhl, G. (1995). Sequential organizing activities of engrailed, hedgehog and decapentaplegic in the Drosophila wing. *Development* **121**, 2265-2278.

Zerial, M. and McBride, H. (2001). Rab proteins as membrane organizers. *Nat. Rev. Mol. Cell Biol.* **2**, 107-117.

Zhu, A. J., Zheng, L., Suyama, K. and Scott, M. P. (2003). Altered localization of Drosophila Smoothened protein activates Hedgehog signal transduction. *Genes Dev.* **17**, 1240-1252.